Title Page

Title:
Drift time corrections based on a practical measurement of the depletion zone to allow accurate and reproducible determination of the reduced mobility of ions in DT-IMS

Running Title (42 characters)
Using depletion zone to correct drift time

Address reprint requests to:

Malcolm Cämmerer
Helmholtz-Zentrum für Umweltforschung GmbH - UFZ
Permoserstr. 15
04318 Leipzig
Germany

malcolm.caemmerer@ufz.de

+49 341 235 1454

Table of Contents/ Abstract Graphic

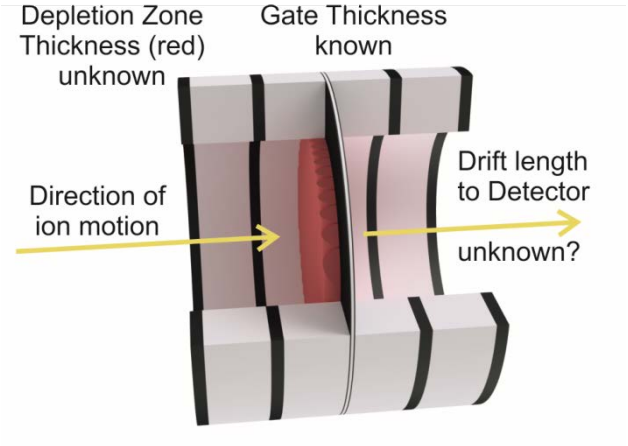

Drift time corrections based on a practical measurement of the depletion zone to allow accurate and reproducible determination of the reduced mobility of ions in DT-IMS

Malcolm Cämmerer, Thomas Mayer and Helko Borsdorf

malcolm.caemmerer@ufz.de

Helmholtz-Zentrum für Umweltforschung GmbH - UFZ
Permoserstr. 15
04318 Leipzig

Abstract: The reduced mobility of an ion is a key parameter for identifying ions and comparing spectra in drift time ion mobility spectrometry (DT-IMS). As the resolution of spectrometers improves, accurate determination of the reduced mobility is increasingly important. The drift time, used to calculate the reduced mobility, is affected by the ion gate and this effect has previously been compensated with a linear correction. These corrections, however, do not allow for changes in the distances that the ions must drift to reach the detector caused by the electric field around the ion gate. As these corrections are a linear correction, non-linearity in the influence of the ion gate may also lead to greater errors. By measuring the length of the depletion zone in front of the ion gate the extra distance travelled by the ions may be corrected for. This measurement also provides the boundary conditions for when a correction to the drift time may be accurately applied. This work shows that the length of the depletion zone can be experimentally measured and that it is consistent for a particular geometry of ion gate.

Keywords: Ion mobility spectrometry, IMS, Error estimation, Optimization, Electric fields

INTRODUCTION

Ion mobility spectrometry is often used for the detection of chemical warfare agents, explosives and drugs [1-4]. The range of applications has however broadened to include (medical) breath analysis [5, 6], process control [7] and food quality and safety assurance [8, 9]. In all of these applications, ions are separated based on the collision diameter, mass and charge of the ion [10]. The intensity and position of a signal peak in the ion mobility spectrum provide information about the concentration of the ion and its identity (collision diameter, mass and charge). It is therefore vital that the position of an ion is accurately and reproducibly determined. In Drift Tube Ion Mobility Spectrometry (DT-IMS) this position is represented by the drift time, t_d [11]. This measurement is also used to calculate the reduced mobility, K_0, of the ion which is defined as the speed of an ion under standardized conditions. The standard conditions are an electric field of 1 V cm^{-1}, a drift gas temperature of 273.15 K and a pressure of 760 Torr [12]. Measurements taken using different instruments under different conditions can then be compared using the reduced mobility of the ions.

$$K_0 = \frac{L}{t_d} \cdot \frac{1}{E} \cdot \frac{p}{760} \cdot \frac{273.15}{T} \qquad (1)$$

As can be seen in Equation 1, variations in the length of the drift region, L; electric field, E; pressure, p; and temperature, T, should all be minimized to ensure an accurate measurement of the reduced mobility [13, 14]. After rigorous minimization of the variation in these parameters it should be possible to report reproducible reduced mobility with an accuracy of 0.01 cm^2 V^{-1} s^{-1} [1, 13, 14]. Whilst further improvements have increased the accuracy by a factor of ten [15], the error in the length of the drift tube remains largely unchanged. These accurate measurements should, in theory at least, allow a database of reduced mobilities of ions to be used to identify the ions present in an unknown ion mobility spectrum when the conditions of the experiment are known [16]. While it has been shown that the theory of reduced mobility should be extended to include the humidity of the gas [17, 18] efforts continue to compensate for the errors when calculating the reduced mobility [13] or reduce them to a minimum [14, 15].

One area that is sometimes overlooked is the effect that the ion gate has on the measurement. The ion gate controls the flow of ions into the drift tube. The ion gate is normally closed by applying a potential to one or more sets of grids placed in close proximity to each other. This applied potential disturbs the electric field in such a way that the ions cannot pass through the ion gate into the drift tube and finally to the detector. A

packet of ions is allowed into the drift tube by opening the ion gate for a short period of time (ca. 5-500 µs). The ion gate is opened either by removing the applied potential and restoring the normal homogenous electric field or, in some cases, by applying an alternate pattern of potentials to the grids [19-21]. The drift time of the ion is the time elapsed between the gate opening (or closing) and the maximum of ion peak in the ion mobility spectrum. As the starting point for the drift time measurement is defined by gate opening or closing, it can easily be seen that choice of reference point (opening or closing) and the time that the ion gate is held open for will have an effect on the drift time measurement. In addition, as a portion of the ion packet is in close proximity to the ion gate as it closes and disturbs the electric field, it is to be expected that the voltage applied to the ion gate will also have an influence on the drift time of the ion. A linear correction of the ion gate pulse width, GPW, and the potential applied to the ion gate has been proposed [22] for both Tyndall-Powell and Bradbury-Nielsen ion gates [23, 24]. This theory defines the correction that should be made to the drift time due to the length of the GPW and the voltage applied to the gate, however it assumes that the drift time changes linearly with respect to these two variables. More recently, it has been shown that the ion gate has a cutting width [25] and that an ion specific gate penetration time, GPT, can be defined. The cutting width is caused by the physical size of the gate is the length of the ion packet lost due to the gate. The gate penetration time is defined by Chen et al. as the minimum GPW to observe a signal to noise ratio for the compound of interest of three [20]. This would lead to a range of GPWs which have no effect on the drift time (as no ions are transmitted through the gate into the drift tube). In addition, the effect of the changing electric field on the ion distribution around opening and closing gates [26] can lead to peak broadening which is most likely due to ions being retarded by the electric field caused by the closed ion gate. When ions near the gate are retarded, this could lead to extended drift times, especially when the majority of ions are close to the ion gate, i.e. at shorter GPWs.

This paper concerns the non-linearity of the drift time measurement measured using Drift Tube Ion Mobility Spectrometer coupled to an Electrospray-Ionization (ESI) source. A wide range of ions were studied to define the areas where non-linear changes to the drift time with respect to GPW can be expected. This leads to recommendations on when corrections may be accurately applied and how this could minimize the error in the drift time measurement.

MATERIAL AND METHODS

A Drift Tube Ion Mobility Spectrometer with Electrospray-Ionization source was mainly used for the experiments. The technical and experimental parameters of the Ion Mobility Spectrometers used are listed in Table 1. The Electrospray-Ionization Source consisted of a PicoCHIP® with a 30µm Fused Silica Emitter (New Objective, Inc., Littleton, USA). Sample Solutions were fed to the emitter from a 100µL Gastight Syringe (Hamilton Company, Reno, USA) using a KDS 100 Syringe Pump (KD Scientific, Hollliston, USA). The PicoCHIP® was connected to a THQ Desktop T2CP 150n High Voltage Supply (iseg, Radeberg, Germany) which also provided the High Voltage connection for the Ion Mobility Spectrometer. The ion gate voltages were controlled by an 33522A Arbitrary Waveform Generator (Agilent Technologies, Santa Clara, USA) and were produced using an open source FET Pulser [27]. The Ion Mobility Spectra were collected using a PicoScope® 3203D (Pico Technology, St. Neots, UK) after being amplified by a Low Noise Current Amplifier (FEMTO® Messtechnik GmbH, Berlin, Germany). The UV-IMS was constructed with identical stainless steel drift rings and MACOR® isolating rings. An identical FET Pulser, Waveform Generator, Signal Amplifier and Oscilloscope were used to collect the data. The 10.6 eV PKS 106 Photoionization Lamp (Heraeus Noblelight GmbH, Hanau, Germany) was mounted on-axis at the start of a short ionization region.

Ethanoic acid, buytric acid (Merck, Darmstadt, Germany), decanoic acid, hexadecanoic acid, octadecanoic acid (Larodan AB, Solna, Sweden) and saccharin (Sigma Aldrich Chemie GmbH, Steinheim, Germany) were dissolved in methanol (Merck, Darmstadt, Germany) and used as test substances using the ESI-IMS. In addition, methyl salicylate (Sigma Aldrich Chemie GmbH, Steinheim, Germany) was used as the test substance for the UV-IMS. All chemicals were at least 99% pure.

Table 1 - IMS Paramters

Parameter	ESI-IMS	UV-IMS
Drift Length	11.3 cm	6.31 cm
Voltage on Drift Tube	- 4972 V	2619 V
Drift Field	- 440 V cm^{-1}	415 V cm^{-1}
Drift Gas	Nitrogen	Synth. Air
Drift Gas Flow	600 ml min^{-1}	500 ml min^{-1}
Drift Gas Temperature	55 °C	40 °C
Drift Gas Pressure	742 – 765 Torr	
Ion Gate Pulse Width	10 - 500 µs	70-225 µs
PicoScope Resolution	500 kHz	
Amplifier Resolution	7 kHz	
Amplifier Gain	10 GV A^{-1}	
Separation of Tyndall-Powell Gate Grids	0.02 cm	
Grid Thickness	0.01 cm	
Total Gate Thickness	0.04 cm	
Voltage applied to Tyndall-Powell Gate	Grid 1 + 10 V Grid 2 - 120 V	- 9.9 V + 118.9 V

RESULTS AND DISCUSSION

Initial Measurements with ESI-IMS

The initial measurements of the variation of drift time with respect to the GPW showed that the current theories mentioned above partially hold. As can be seen in Figure 1, the drift time of the ions varies

linearly with the GPW at longer drift times. At GPWs under a certain threshold, it can also be seen that the gate has a cutting width or gate penetration time. Curiously, between these two extremes, the drift time falls before reaching a minimum and then rising into range where the linear relationship can be seen. As the position of the gate penetration time, the minimum drift time and the start of the linear correlation between drift time and GPW all differed depending on the identity of the ion, the mathematical model used to describe these phenomena was based on the ion mobility.

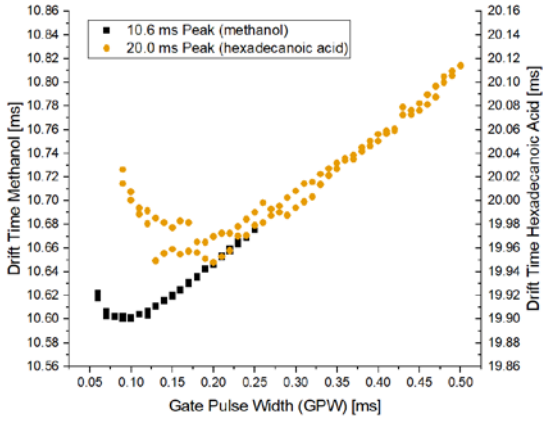

Figure 1. Variation of the drift time of negative methanol and hexadecanoic acid ions with respect to the GPW. All peaks greater than 20 times baseline standard deviation.

Mathematical Model

When the ion gate closes, some of the ions between the grids will not be transmitted to the drift tube [25]. There are also depletion zones that exist in front of the ion gate due to the voltage applied to the grids of the ion gate [28]. The length of the ion packet in the drift tube, L_{real}, is then dependent on the maximum length of the ion packet, L_{max}, and the length of the depletion zone, $L_{depletion}$. These lengths are shown in Figure 2. In this work, Tyndall-Powell gates with a physical width of 0.04cm were used. This means that $L_{depletion}$ measured in this work should be at least 0.04cm.

This depletion zone describes both the area in front of ion gate where ions are depleted before the gate opens and the area within the gate where ions are not transmitted to the drift tube when the gate closes. Assuming a uniform concentration of ions, c, in the ionization region with a cross-sectional area, A, the number of ions found in the drift tube, n, after the gate closes will be:

$$n = c \cdot A \cdot L_{real} \quad (2)$$

$$n = c \cdot A . L_{max} - c \cdot A \cdot L_{depletion} \quad (3)$$

$$L_{max} = K \cdot E \cdot t_{GPW} \quad (4)$$

From Equation 4, the maximum length of the ion packet is proportional to the GPW, t_{GPW}. By substituting this into Equation 3 and also assuming that the number of ions in the drift tube is equal to the area of a peak with that mobility, S_K, multiplied by an instrument specific factor, f, the relationship becomes:

$$S_K \cdot f = c \cdot A \cdot K \cdot E \cdot t_{GPW} - c \cdot A \cdot lL_{depletion} \quad (5)$$

When the S_K is plotted against the $K \cdot E \cdot t_{GPW}$, the length of the depletion zone can be calculated from the value at the x-axis where the S_K is zero as shown in Equation 6 and 7:

$$0 = c \cdot A \cdot K \cdot E \cdot t_{GPW} - c \cdot A \cdot L_{depletion} \quad (6)$$

$$L_{depletion} = K \cdot E \cdot t_{GPW} \quad (7)$$

As this model assumes a linear variation in signal intensity with the GPW, the x-intercept should be calculated using a linear regression of the signal area over a wide range of GPWs. The length of depletion zone is now considered to be an instrument specific factor which can be used to calculate the gate penetration time, t_{GPT}, for any ion. Equation 8 therefore provides an alternate definition of the gate penetration time which is instrument specific:

$$t_{GPT} = \frac{L_{depletion}}{K \cdot E} \quad (8)$$

This calculation can be performed for any new ion with a known reduced mobility without the need for test measurements to find the point where the peak intensity is three times the noise in the spectrum [20]. This prevents the user from selecting an unrealistically short GPW which is less than t_{GPT} when measuring larger ions.

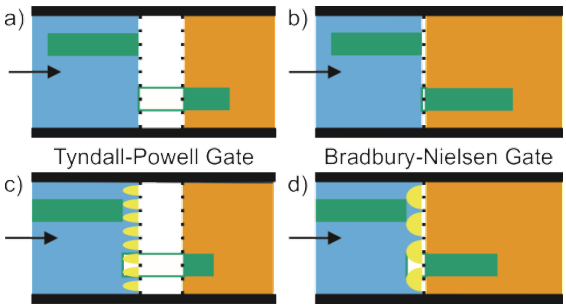

Figure 2. Schematic depiction of an ion gate in an ion mobility spectrometer. A Tyndall-Powell gate is shown in a) and c) whilst a Bradbury-Nielsen gate is shown in b) and d). The color coding in all diagrams is as follows: Blue - ionization region in front of the ion gate; orange - drift tube after the ion gate; yellow - depletion zone caused by the voltage applied to a closed ion gate; green bar - an ion packet with length, L_{max}. The upper ion packet in a)-d) is aligned to the closest point to the ion gate. The lower ion packet in a)-d) is aligned to the same point and the ions lost due to the ion gate with length, $L_{depletion}$, are represented by a green frame. The length of the ion packet in the drift tube, L_{real}, is shown by the green bar in the bottom right of each picture.

Depletion Zone Measurements with ESI-IMS

As the depletion zone is caused by the electric field applied to the gate, the length of the depletion zone should be constant for all ions at a particular ratio of gate voltage to electric field.

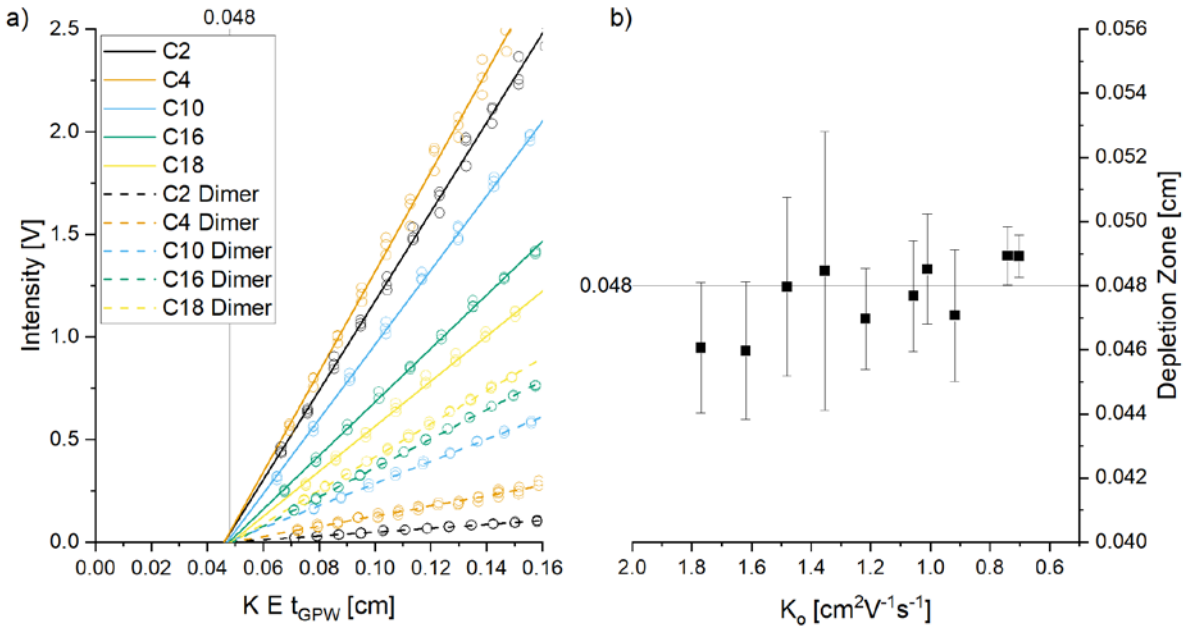

Figure 3. Depletion zone measurements for saturated fatty acids of different chain lengths (C2- C18). a) The variation of peak intensity with respect to GPW is used to calculate the depletion zone length for these ion. b) These depletion zone lengths with respect to the reduced mobility of the ions. The depletion zone length of 0.048 ± 0.003 cm is the average length for all the ions in these graphics and is marked in both.

Although the mobility of the ion and the electric field are in Equation 7, the depletion zone cannot be measured but varying these terms as they also influence the concentration of ions in the ionization region. The depletion zone should be measured by varying the GPW and measuring the intensity of the ion peak. The length of the depletion zone should be constant for ions of different mobilities, at different concentrations and in different electric fields whilst retaining the ratio to gate voltage. Changing the ratio of electric field and the gate voltage should however change the length of the depletion zone as shown in previous studies [28, 29]. In the following measurements, the peaks were assumed to be perfect Gaussian functions and the peak height was taken as a proxy for the peak area. The drift time and intensity of a wide range of ion peaks were measured. These measurements form the basis of the depletion zone measurement. As the GPW was varied, the intensity and position of the peak were measured and the peak intensity plotted against K E t_{GPW}. The length of the depletion zone was then determined according to Equation 6 and 7 and the standard deviation of the linear regression was calculated according to DIN 32645, “Chemical analysis - Decision limit, detection limit and determination limit under repeatability conditions - Terms, methods, evaluation” (DIN e.V., Berlin, Germany).

Reduced Mobility

A range of saturated fatty acids were measured and, where possible, the dimer ions were also measured. The GPW was then varied for each fatty acid so that the length of the depletion zone could be calculated. As shown in Figure 3, the average length of the depletion zone (0.048 ± 0.003cm) is within one standard deviation of the length measured for all the ions shown except the dimer ions of hexadecanoic and octadecanoic acid (C16 and C18 dimer, $K_o < 0.8$ $cm^2V^{-1}s^{-1}$).

Electric Field

The drift time and intensity of the saccharin peak (1 ng μL^{-1}) was measured at a range of electric field strengths and the voltage applied to the ion gate was adjusted to retain the same conditions relative to the electric field. Very low electric field strengths were not used as high accuracy measurements have revealed that the ion mobility increases slightly with decreasing electric field [30]. The GPW was then varied for each electric field setting which allowed the length of the depletion zone to be calculated. In these experiments, the average length of the depletion zone, shown in Figure 4 to be 0.048 ± 0.002 cm, is within one standard deviation of the length measured at all electric field strengths.

Concentration

Saccharin solutions covering a range of concentrations over two orders of magnitude were used to confirm if the length of the depletion zone is independent of the concentration of the ions used. At low concentrations (0.1 – 11 µmol L^{-1}), the average length of the depletion zone was shown to be within one standard deviation of all the measurements. Although Figure 5a) shows that the measurement of the depletion zone was shorter at higher concentrations, it can be seen in Figure 5b) that this highly concentrated solution is outside the range of concentrations which show a linear response to increasing concentration.

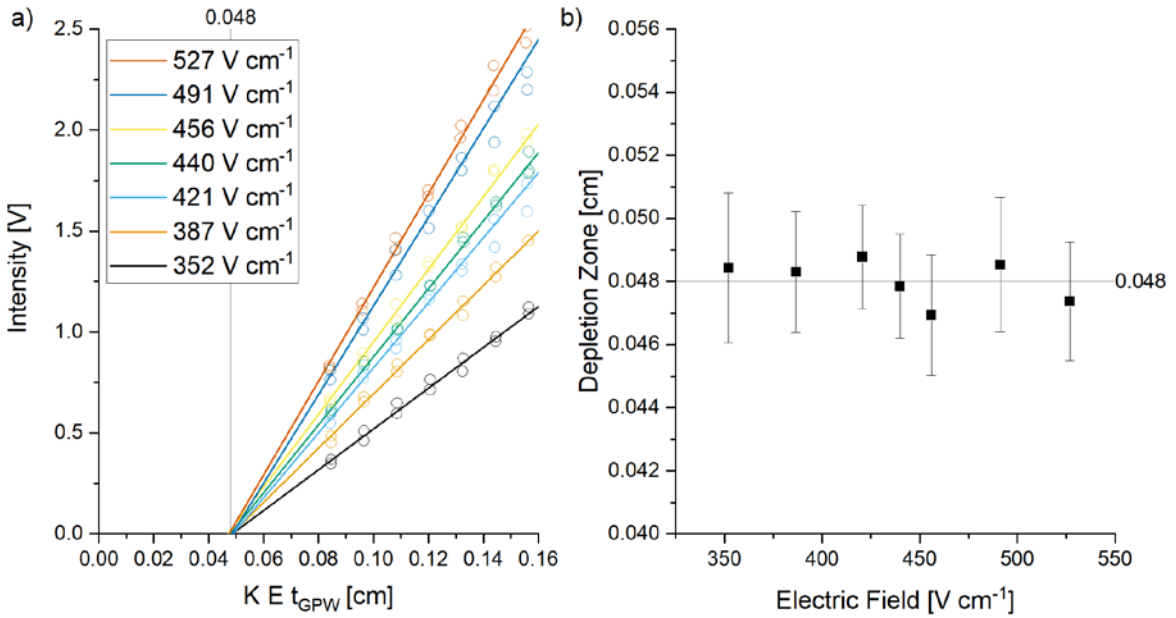

Figure 4. Depletion zone measurements for the saccharin peak for a range of electric field strengths applied to the drift tube. a) The variation of peak intensity with respect to GPW is used to calculate the depletion zone length for each electric field strength. b) These depletion zone lengths are shown with respect to the reduced mobility of the ions. The depletion zone length of 0.048 ± 0.002 cm is the average length for all the ions in these graphics and is marked in both.

As increasing space charge can lead to peak broadening [31], this reduction in the length of the depletion zone could be due to increasing space charge. This would require further investigation at higher levels of precision to confirm this effect.

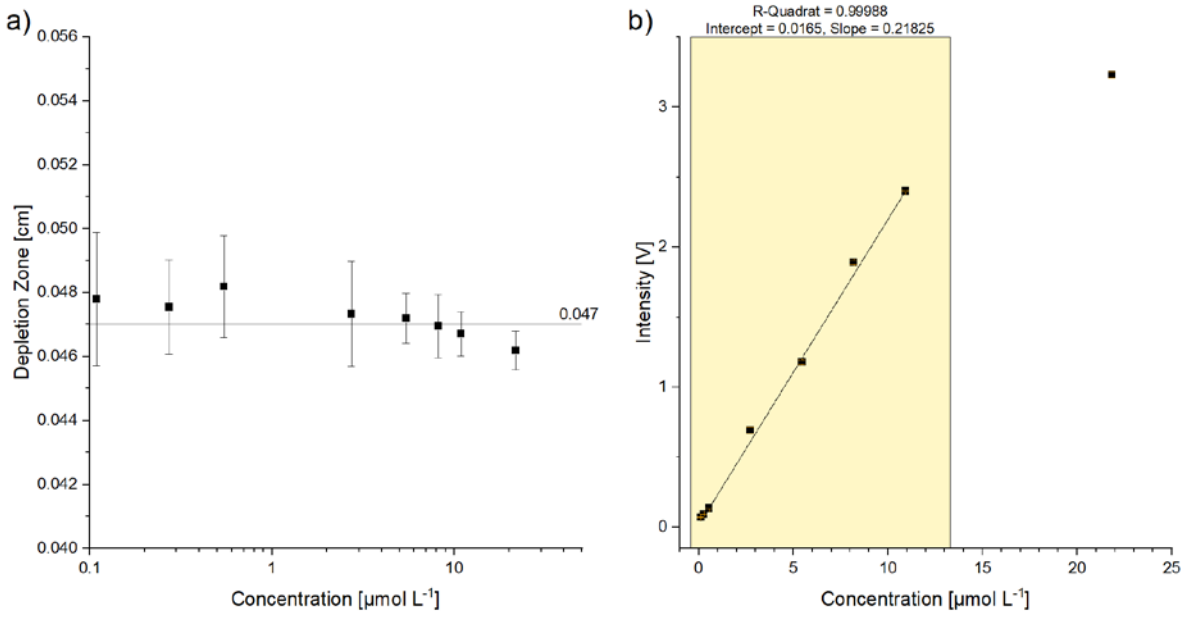

Figure 5. Depletion zone measurements for saccharin ions at a variety of concentrations. a) The variation of the depletion zone with respect to the concentration shows all but one measurement are within one standard deviation of the average depletion zone length of 0.047 ± 0.002 cm. b) The variation of peak intensity with respect to concentration with the range of linear response marked by the yellow box. A linear response to increasing concentration was observed over 2 orders of magnitude.

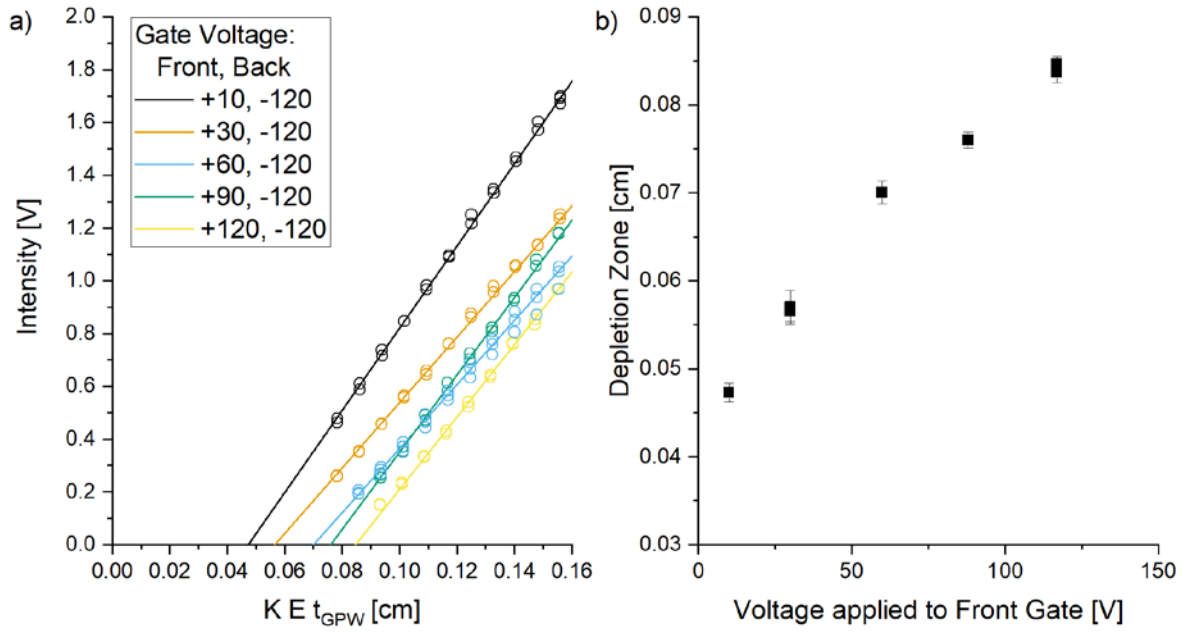

Figure 6. Depletion zone measurements for the saccharin peak for a range of voltages applied to the front set of gate wires. a) The variation of peak intensity with respect to GPW is used to calculate the depletion zone length for these ion. b) These depletion zone lengths are shown with respect to the voltage on the front gate.

Voltage on the Ion Gate

As the voltage on the front set of gate wires increases, the length of the depletion zone would be expected to increase. As the voltage on the back set of gate wires, i.e. the set of gate wires closest to the detector, was kept constant, any increase to the length of the depletion zone is assumed to be in front of the grid, as shown in Figure 2. As seen in Figure 6, the depletion zone increases in length as the voltage applied to the front set of grid wires increase.

Depletion Zone Measurements with UV-IMS

To remove any doubt, that this phenomenon is somehow related to the electrospray ionization source, the same experiments were carried out on a shorter (see Table 1) IMS using an Ultraviolet lamp as the ionization source.

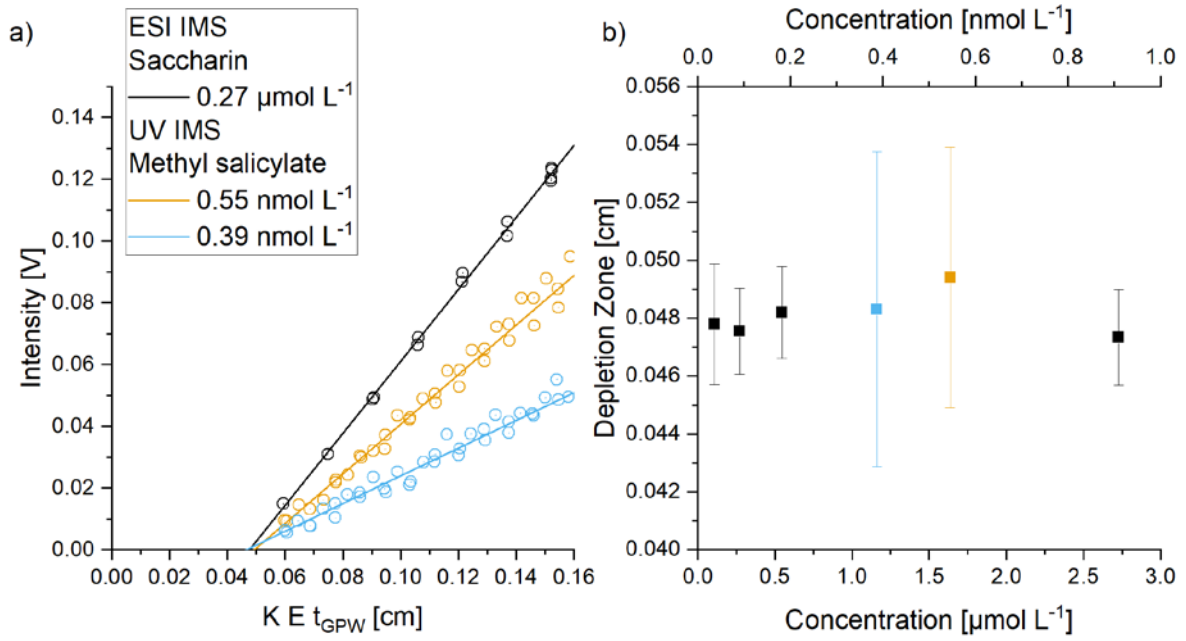

Figure 7. Depletion zone measurements for negative saccharin ions produced by electrospray ionization and for positive methyl salicylate ions produced by photoionization. a) The variation of peak intensity with respect to GPW is used to calculate the depletion zone length for these ion. b) These depletion zone lengths are shown with respect to the concentrations of these ions.

Care was taken to ensure that the equipment used was identical but not the same machine to eliminate systematic errors caused by the equipment. The spectra for the positive ions were measured using an identical Picoscope 3203D after amplification with a Low Noise Current Amplifier. An identical Tyndall-Powell style gate was, again, controlled by a 33522A Arbitrary Waveform Generator and the voltages for the ion gate produced using an identical open source FET Pulser. The electric field applied to the drift region was set to 415 V cm^{-1} which lead to the gate voltages being set to -9.9V and +118.9V.

As shown in Figure 7, the length of the depletion zone when applying the same ratio of voltages to the same geometry remains constant for both ionization sources and IMS drift tube lengths. The increase in the standard deviation for the measurements using the UV IMS is due to the reduced signal intensity compared to that measured using the ESI IMS.

Drift Time Corrections

To calculate the corrected drift time, $t_{d\ corr.}$, the drift time should be plotted with respect to the GPW as shown in Figure 8. In the case of the ions shown in Figure 1 and Figure 8, the gate penetration times calculated from Equation 8 are 60µs for the methanol ion and 114 µs for the hexadecanoic acid ion. The region in which the drift time linearly varies with respect to the GPW is taken to be at GPWs greater than three times the gate penetration times (GPT). These areas are marked in Figure 8 and define the data which may be used to calculate the α correction term proposed by Spangler [22] according to Equation 10.

$$t_d = \frac{t_{GPW}}{\alpha} + t_{d\ corr.} \qquad (10)$$

Figure 8 is therefore the graphical representation of Equation 10 whereby the drift time of the ion, t_d, is plotted with respect to the GPW. The slope of the linear regression is equal to 1/α and $t_{d\ corr}$ can be taken from the y-intercept of the regression. As in Spangler's work, the α correction term will depend on whether the rising or falling edge of the gate control signal is used to start the timing. The main difference to previous corrections is that data may only be used to calculate a reduced mobility when the GPW is sufficiently long.

Case 1: Depletion Zone is added to the drift length

After the corrected drift time has been calculated from Equation 10, the length used for the reduced mobility measurements is the length of the drift tube plus that of the depletion zone. This means that the ions drift from the start of the gate penetration zone to the detector in the time between the start of the timing signal and the time at the maximum of the peak. Equation 1 is therefore modified as shown below:

$$K_0 = \frac{L_{drift} + L_{depletion}}{t_{d\ corr.}} \cdot \frac{1}{E} \cdot \frac{p}{760} \cdot \frac{273.15}{T} \qquad (11)$$

.

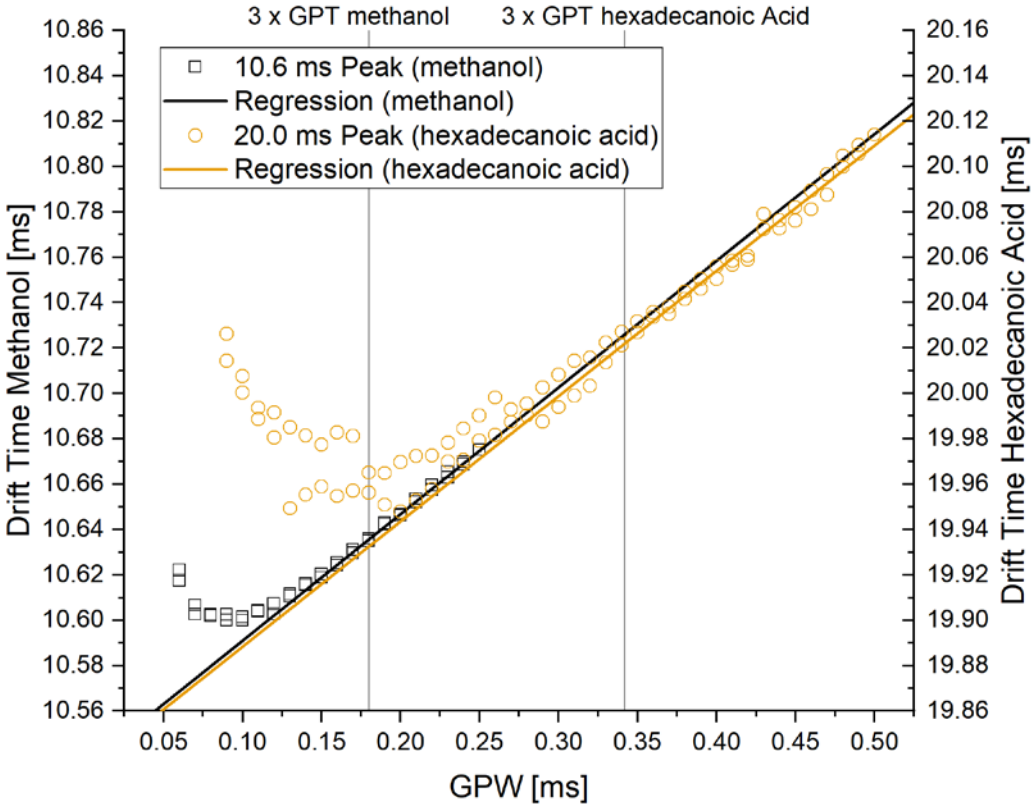

Figure 8. Variation of the drift time of negative methanol and hexadecanoic acid ions with respect to the effective GPW of the Tyndall-Powell gate as shown in Figure 1. Linear Regression of the data is shown for GPWs greater than three times the GPT. All peaks greater than 20 times baseline standard deviation.

Case 2: Gate Penetration Time is subtracted from the drift time

As the length of the depletion zone can also be used to calculate the gate penetration time for a specific ion mobility, the same correction may be applied by subtracting the gate penetration time from the corrected drift time. Here the ions drift from the start of the drift tube to the detector in the time between the gate penetration time and the time at the maximum of the peak. Equation 1 is therefore modified as shown below:

$$K_0 = \frac{L_{drift}}{t_{d\,corr.} - t_{GPT}} \cdot \frac{1}{E} \cdot \frac{p}{760} \cdot \frac{273.15}{T} \qquad (12)$$

Limits of the drift time correction and reduced mobility values

The fact that drift times vary in a non-linear manner with respect to the GPW emphasizes the need for caution when applying a correction to the drift time. The corrected drift time should only be calculated based on data points taken when the drift varies linearly with the GPW. As seen in Figure 8, this area is estimated to start when the GPW is three times the gate penetration time for that ion. This ensures that the ion cloud is suitably far from the ion gate (the front of the ion cloud will be at approximately twice the length of the depletion zone) which therefore minimizes the effect of the gate on the ion cloud proposed by Siems et al. [26]. This restriction on the usage of a correction is shown in Figure 8a whereby the reduced mobility is not calculated when the GPW is too short.

The use of the length of the depletion zone to calculate the gate penetration time and the minimum GPW for accurate measurements is novel. Previously the gate penetration time was taken to be the minimum GPW for observing a signal with a signal to noise ratio of three [20]. As the signal to noise ratio improves and small peaks stand out from the noise, for example through improvements to the signal amplifier, the risk of evaluating peaks at very low effective GPWs increases. This could lead to incorrect application of corrections. All peaks shown in all the graphics were greater than three times the noise level showing that the new definition of GPT leads to a longer GPT. This new definition for the minimum GPW should also be considered when applying a correction for the peak intensity [25] as the peak intensity was seen to vary non-linearly at low effective GPWs.

The effect of the front gate on the reduced mobility is also minimized, as seen in Figure 8b. Variations in the voltage on the rear gate which affect post gate compression of the ion packet are, however, not eliminated using this correction.

Conclusion

Average length of the depletion zone was determined to be 0.048 ± 0.002 cm for all ions measured in this study. This was consistent over a range of concentrations, ion mobilities, chemical structures, electric field strengths and ionization sources. The fact that the length of the depletion zone was consistent when using the same ion gate in different ion mobility spectrometers (ESI-IMS and UV-IMS) shows that this length is determined by the gate dimensions and voltages. This length can therefore be applied to all measurements using this IMS when the same voltages are applied to the ion gate. A minimum GPW for all drift times in the ion mobility spectrum can then be defined and the drift times corrected where appropriate. Without the use of the correction in this work, the variation in corrected reduced mobilites can be significantly greater than the 0.1% error shown by the highest quality IMS measurements (see Figure 9)[15].

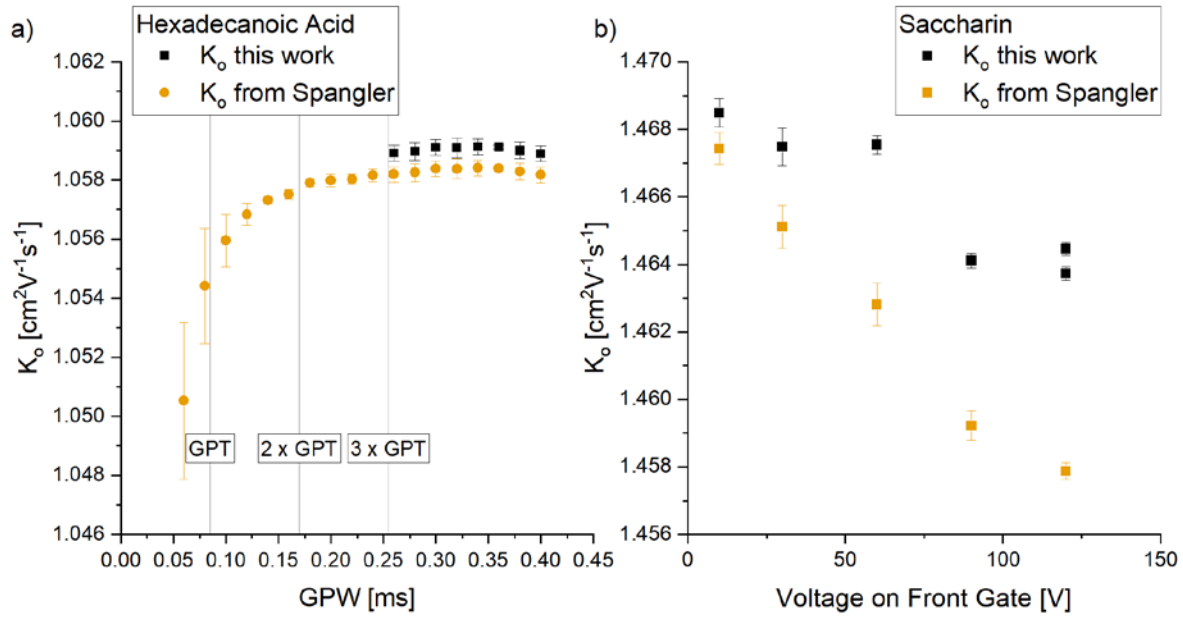

Figure 9. Reduced mobilities calculated using the correction and limits to the correction proposed in this work and also using the correction proposed by Spangler [22]. a) Multiples of the GPT for the hexadecanoic acid ion are marked and, according to this work, a correction may be applied at GPWs greater than three times the GPT. All points greater than 5 times the baseline noise. b) The reduced mobility of saccharin ion with respect to the voltages applied to the front gate.

The gate penetration time can now be defined using the length of the depletion zone as shown in Equation 8. This allows experiments to be more easily planned as this can be calculated for an ion with a known mobility measured using a spectrometer with a known depletion zone. As shown in Figure 9, the selected GPW should be greater than three times GPT which is the proposed boundary condition. For experiments using a reference substance, this must be satisfied for both the reference as well as the compound of interest.

The length of the depletion zone can further be used to assess the effectiveness of an ion gate and evaluate any proposed changes to its design or usage. An ideal gate shows no discrimination and ions of all ion mobilites are transmitted through the gate into the drift region equally. The length of the depletion zone in such an ideal gate would be zero. The ability to measure the real changes to this length will therefore allow computational models to be more effectively designed and used in this process.

Finally the fact that this correction reduces the influence of the ion gate's electrical field in front of the gate should allow further study of post gate compression effects. If post gate effects are not present, the boundary conditions shown in Figure 8 are also not required as the reduced mobility would be constant for all GPW. Whilst an inhomogeneity in the effective electric field was presented as a possible source for the changes in reduced mobility at low E/N, the effect of the ion gate was discounted based on the theoretical model of the 2 gate system used [30]. The measurements presented in this article can be used to prove whether the 2 gate system eliminates the effect of the ion gate, i.e. the length of the depletion zone is equal for both gates. Further efforts are therefore required to measure the length of the depletion zone for different ion gate systems and establish what boundary conditions must be fulfilled to allow accurate measurement of the reduced mobility of an ion.

Conflicts of Interest

The authors declare that there is no conflict of interest.

AUTHOR INFORMATION

Corresponding Author

Malcolm Cämmerer
Helmholtz-Zentrum für Umweltforschung GmbH - UFZ
Permoserstr. 15
04318 Leipzig
malcolm.caemmerer@ufz.de
+49 341 235 1454

Author Contributions

The manuscript was written through contributions of all authors.

ACKNOWLEDGMENT

This research was supported by the Sächsische Aufbaubank - Förderbank - (SAB) using funds provided by the European Union and the Free State of Saxony (Application Number: 100352242, Approved: 09.05.2019).

REFERENCES

1. Eiceman, G.A., Karpas, Z., Hill, H.H. Taylor & Francis Group, (2013)
2. Wu, C., Siems, W.F., Hill, H.H.: Secondary electrospray ionization ion mobility spectrometry/mass spectrometry of illicit drugs. Anal Chem. **72**, 396-403 (2000)
3. Armenta, S., Esteve-Turrillas, F.A., Alcala, M.: Analysis of hazardous chemicals by "stand alone" drift tube ion mobility spectrometry: A review. Anal Methods-Uk. (2020)
4. Buryakov, I.A.: Express analysis of explosives, chemical warfare agents and drugs with multicapillary column gas chromatography and ion mobility increment spectrometry. J Chromatogr B. **800**, 75-82 (2004)
5. Baumbach, J.I.: Ion mobility spectrometry coupled with multi-capillary columns for metabolic profiling of human breath. J Breath Res. **3**, 1-16 (2009)
6. Christiansen, A., Davidsen, J.R., Titlestad, I., Vestbo, J., Baumbach, J.: A systematic review of breath analysis and detection of volatile organic compounds in COPD. J Breath Res. **10**, 034002 (2016)
7. Baumbach, J.I.: Process analysis using ion mobility spectrometry. Anal Bioanal Chem. **384**, 1059-1070 (2006)
8. Vautz, W., Zimmermann, D., Hartmann, M., Baumbach, J.I., Nolte, J., Jung, J.: Ion mobility spectrometry for food quality and safety. Food Addit Contam. **23**, 1064-1073 (2006)
9. Wang, S., Chen, H., Sun, B.: Recent progress in food flavor analysis using gas chromatography–ion mobility spectrometry (GC–IMS). Food Chem. **315**, 126158 (2020)
10. Revercomb, H.E., Mason, E.A.: Theory of Plasma Chromatography Gaseous Electrophoresis - Review. Anal Chem. **47**, 970-983 (1975)
11. Hill, H.H., Siems, W.F., Stlouis, R.H., Mcminn, D.G.: Ion Mobility Spectrometry. Anal Chem. **62**, A1201-A1209 (1990)
12. Cohen, M.J., Karasek, F.W.: Plasma Chromatography - a New Dimension for Gas Chromatography and Mass Spectrometry. J Chromatogr Sci. **8**, 330-& (1970)
13. Vautz, W., Bödeker, B., Baumbach, J., Bader, S., Westhoff, M., Perl, T.: An implementable approach to obtain reproducible reduced ion mobility. Int J Ion Mobility Spectrom. **12**, 47-57 (2009)
14. Crawford, C.L., Hauck, B.C., Tufariello, J.A., Harden, C.S., McHugh, V., Siems, W.F., Hill, H.H.: Accurate and reproducible ion mobility measurements for chemical standard evaluation. Talanta. **101**, 161-170 (2012)
15. Hauck, B.C., Siems, W.F., Harden, C.S., McHugh, V.M., Hill, H.H.: High Accuracy Ion Mobility Spectrometry for Instrument Calibration. Anal Chem. **90**, 4578-4584 (2018)
16. Shumate, C., Stlouis, R.H., Hill, H.H.: Table of Reduced Mobility Values from Ambient Pressure Ion Mobility Spectrometry. Journal of Chromatography. **373**, 141-173 (1986)
17. Izadi, Z., Tabrizchi, M., Borsdorf, H., Farrokhpour, H.: Humidity Effect on the Drift Times of the Reactant Ions in Ion Mobility Spectrometry. Anal Chem. **91**, 15932-15940 (2019)
18. Mayer, T., Borsdorf, H.: Accuracy of Ion Mobility Measurements Dependent on the Influence of Humidity. Anal Chem. **86**, 5069-5076 (2014)
19. Chen, C., Tabrizchi, M., Li, H.: Ion gating in ion mobility spectrometry: Principles and advances. TrAC Trends in Analytical Chemistry. **133**, 116100 (2020)
20. Chen, C., Chen, H., Li, H.Y.: Pushing the Resolving Power of Tyndall-Powell Gate Ion Mobility

Spectrometry over 100 with No Sensitivity Loss for Multiple Ion Species. Anal Chem. **89**, 13398-13404 (2017)

21. Zühlke, M., Zenichowski, K., Riebe, D., Beitz, T., Löhmannsröben, H.G.: An alternative field switching ion gate for ESI-ion mobility spectrometry. Int J Ion Mobility Spectrom. **20**, 67-73 (2017)
22. Spangler, G.E.: Theory and Technique for Measuring Mobility Using Ion Mobility Spectrometry. Anal Chem. **65**, 3010-3014 (1993)
23. Tyndall, A.M., Powell, C.F., Chattock, A.P.: The mobility of ions in pure gases. Proceedings of the Royal Society of London. Series A, Containing Papers of a Mathematical and Physical Character. **129**, 162-180 (1930)
24. Bradbury, N.E., Nielsen, R.A.: Absolute Values of the Electron Mobility in Hydrogen. Phys Rev. **49**, 388-393 (1936)
25. Tabrizchi, M., Shamlouei, H.R.: Relative transmission of different ions through shutter grid. Int J Mass Spectrom. **291**, 67-72 (2010)
26. Siems, W.F., Wu, C., Tarver, E.E., Hill, H.H., Larsen, P.R., Mcminn, D.G.: Measuring the Resolving Power of Ion Mobility Spectrometers. Anal Chem. **66**, 4195-4201 (1994)
27. Garcia, L., Saba, C., Manocchio, G., Anderson, G.A., Davis, E., Clowers, B.H.: An open source ion gate pulser for ion mobility spectrometry. Int J Ion Mobility Spectrom. **20**, 87-93 (2017)
28. Chen, H., Chen, C., Li, M., Wang, W., Jiang, D., Li, H.: Achieving high gating performance for ion mobility spectrometry by manipulating ion swarm spatiotemporal behaviors in the vicinity of ion shutter. Anal Chim Acta. **1052**, 96-104 (2019)
29. Tadjimukhamedov, F.K., Puton, J., Stone, J.A., Eiceman, G.A.: A study of the performance of an ion shutter for drift tubes in atmospheric pressure ion mobility spectrometry: Computer models and experimental findings. Rev Sci Instrum. **80**, - (2009)
30. Hauck, B.C., Siems, W.F., Harden, C.S., McHugh, V.M., Jr., H.H.H.: E/N effects on K0 values revealed by high precision measurements under low field conditions. Rev Sci Instrum. **87**, 075104 (2016)
31. Mariano, A.V., Su, W., Guharay, S.K.: Effect of space charge on resolving power and ion loss in ion mobility spectrometry. Anal Chem. **81**, 3385-3391 (2009)